The Astrophysical Journal, 646:351–357, 2006 July 20

TESTING THE CURVATURE EFFECT AND INTERNAL ORIGIN OF GAMMA-RAY BURST PROMPT EMISSIONS AND X-RAY FLARES WITH *SWIFT* DATA

E. W. Liang,[1,2] B. Zhang,[1] P. T. O'Brien,[3] R. Willingale,[3] L. Angelini,[4] D. N. Burrows,[5] S. Campana,[6] G. Chincarini,[6,7] A. Falcone,[5] N. Gehrels,[4] M. R. Goad,[3] D. Grupe,[5] S. Kobayashi,[8] P. Mészáros,[5,9] J. A. Nousek,[5] J. P. Osborne,[3] K. L. Page,[3] and G. Tagliaferri[6]

Received 2006 February 6; accepted 2006 March 24

ABSTRACT

The X-ray light curves of many GRBs have a steep tail following the gamma-rays and have some erratic flares. We assume that these tails and flares are of "internal" origin and that their decline behaviors are dominated by the curvature effect. This effect suggests that the decay slope of the late steep decay part of the light curves is $\alpha = 2 + \beta$, where β is the X-ray spectral index. We present a self-consistency test for this scenario with a sample of 36 prompt emission tails/flares in 22 light curves observed by the *Swift* XRT. We derive the zero time (t_0) for each steep decay component by fitting the light curves with the constraint of $\alpha = 2 + \beta$. Our results show that the $t_0$values of the prompt emission tails and the tails of well-separated flares are self-consistent with the expectation of the internal dissipation models, indicating that each X-ray flare forms a distinct episode of the central engine activity and the central engine remains active after the prompt emission is over, sometimes up to $\sim$1 day after the GRB trigger. This challenges the conventional models and calls for new ideas to restart the central engine. We further show that the onset time of the late central engine activity does not depend on the GRB duration. We also identify a minority group of GRBs whose combined BAT-XRT light curves are smoothly connected, without an abrupt transition between the prompt emission and the afterglow. These GRBs may have an external origin for both the prompt emission and the afterglow.

Subject headings: gamma rays: bursts — methods: statistical

Online material: color figures

1. INTRODUCTION

The successful launch and operation of the *Swift* mission (Gehrels et al. 2004) have led to several important discoveries (e.g., Tagliaferri et al. 2005; Burrows et al. 2005; Gehrels et al. 2005; Fox et al. 2005; Barthelmy et al. 2005a; Roming et al. 2006; Cusumano et al. 2006a). Combined analyses of the early data from the Burst Alert Telescope (BAT) and the X-Ray Telescope (XRT) for a large sample of bursts (Nousek et al. 2006; O'Brien et al. 2006) reveal a canonical X-ray afterglow light curve characterized by five components (Zhang et al. 2006a; see also Nousek et al. 2006): a steep decay component associated with the GRB prompt emission tail, a shallow decay component likely due to refreshing of the forward shock, a normal decay component, a possible steep decay component following a jet break, as well as one or more X-ray flares. These new data provide unprecedented information to unveil the nature of these mysterious explosions.

One of the outstanding problems in the pre-*Swift* era concerned the emission site of the prompt gamma-ray emission. It is generally believed that GRB prompt emission originates at a distance internal to the fireball deceleration radius. The most widely discussed scenario is the internal shock model (Rees & Mészáros 1994; Kobayashi et al. 1997; Daigne & Mochkovitch 1998), but magnetic dissipation at an internal radius is also possible (e.g., Usov 1992; Thompson 1994; Drenkhahn & Spruit 2002; Giannios & Spruit 2006). The broadband afterglows, on the other hand, are produced by the external shocks when the fireball is decelerated by the ambient medium (Mészáros & Rees 1997; Sari et al. 1998). This "internal+external shock" model suggests that the prompt emission and the afterglow involve two distinct processes at two different emission sites. Alternatively, it has been argued that both the GRB prompt emission and the afterglows are produced in external shocks, provided that the immediate medium near the burster is clumpy enough (Dermer & Mitman 1999, 2004). The evidence collected in the pre-*Swift* era cannot conclusively differentiate between the internal and the external models (see Zhang & Mészáros 2004 for a critical review on the successes and limitations of both models). It is one of the scientific goals of the *Swift* to pin down the emission site of GRB prompt emission using early afterglow data.

The steep decay component commonly existing in early X-ray afterglows (Tagliaferri et al. 2005; Barthelmy et al. 2005b; Cusumano et al. 2006b; Vaughan et al. 2006) has been generally interpreted as the tail of the prompt emission (Zhang et al. 2006a; Nousek et al. 2006; Panaitescu et al. 2006; Yamazaki et al. 2006; Lazzati & Begelman 2006). This component strongly suggests that the prompt emission and the afterglow are two distinct components, which supports the internal origin of the prompt emission (Zhang et al. 2006a; cf. C. D. Dermer, 2006, in preparation). The distinct X-ray flares typically show rapid rise and fall, with the ratio of the variability timescale and the epoch of the flare typically much less than unity, i.e., $\delta t/t \ll 1$ (Burrows et al. 2005;

[1] Physics Department, University of Nevada, Las Vegas, NV 89154; lew@physics.unlv.edu, bzhang@physics.unlv.edu.
[2] Department of Physics, Guangxi University, Nanning 530004, China.
[3] Department of Physics and Astronomy, University of Leicester, Leicester LE1 7RH, UK.
[4] NASA Goddard Space Flight Center, Greenbelt, MD 20771.
[5] Department of Astronomy and Astrophysics, Pennsylvania State University, University Park, PA 16802.
[6] INAF—Osservatorio Astronomico di Brera, via Bianchi 46, I-23807 Merate, Italy.
[7] Dipartimento di Fisica, Universitá degli studi di Milano-Bicocca, Piazza delle Scienze 3, 20126 Milan, Italy.
[8] Astrophysics Research Institute, Liverpool John Moores University, Twelve Quays House, Birkenhead, CH41 1LD, UK.
[9] Department of Physics, Pennsylvania State University, University Park, PA 16802.

Falcone et al. 2006; Romano et al. 2006). Burrows et al. (2005) proposed in their discovery paper that the flares are also produced in internal shocks at later times, which requires reactivation of the GRB central engine. Zhang et al. (2006a) performed more detailed analysis of various possible scenarios and concluded that the late internal dissipation model is the correct interpretation of X-ray flares. Similar conclusions have been also drawn by Ioka et al. (2005), Fan & Wei (2005), Falcone et al. (2006), and Romano et al. (2006) (see Piro et al. 2005; C. D. Dermer 2006, in preparation).

An important clue to diagnose the internal origin of the prompt emission and the X-ray flares is provided by the steep decay components following the prompt emission and the flares. These mark the sudden cessations of the emission, and the rapid decays are due to the observer receiving the progressively delayed emission from higher latitudes—the so-called curvature effect (Kumar & Panaitescu 2000; Dermer 2004; Zhang et al. 2006a; Fan & Wei 2005; Panaitescu et al. 2006; Dyks et al. 2006; Wu et al. 2006). The internal emission could be either from conventional internal shocks (Rees & Mészáros 1994; Kobayashi et al. 1997; Daigne & Mochkovitch 1998) or from magnetic dissipation at an internal radius (e.g., Usov 1992; Thompson 1994; Drenkhahn & Spruit 2002; Giannios & Spruit 2006). Usually the detected emission contains the contributions from many emission episodes (e.g., emission from many internal shocks or magnetic dissipation regions). Each emission episode is expected to be followed by a curvature effect tail after the cessation of the emission (e.g., shock crosses the shell or magnetic reconnection finishes). For highly overlapping emission episodes (e.g., the prompt emission), a curvature tail is usually buried beneath the rising light curve of another episode, so that it is difficult to observe a clear curvature effect signature. Although extensive studies have been made of the curvature effect in the prompt emission phase (Fenimore et al. 1996; Sari & Piran 1997; Ryde & Petrosian 2002; Norris 2002; Kocevski et al. 2003; Qin et al. 2004; Shen et al. 2005; Qin & Lu 2005), no conclusive evidence supporting this effect has been presented (e.g., Kocevski et al. 2003).

A clear, testable prediction of the curvature effect when the viewing angle is larger than the $1/\Gamma$ cone (where Γ is the bulk Lorentz factor of the emission region) is that the temporal decay index α should be related to the spectral index β by the expression (Kumar & Panaitescu 2000)

$$\alpha = 2 + \beta, \tag{1}$$

where the convention $F_\nu \propto t^{-\alpha}\nu^{-\beta}$ is adopted. This relation is valid under the following assumptions: (1) that there is a sharp drop off in the injection of accelerating electrons at a certain radius, after which the electrons cool adiabatically; (2) that no spectral break energy crosses the observational band during the epoch of decay; and (3) that the observational band is above the cooling frequency. When these conditions are satisfied, such a relation is rather robust, regardless of the fireball history (e.g., Zhang et al. 2006a; Fan & Wei 2005; Dyks et al. 2006; Wu et al. 2006) and depends only on the jet structure when the line of sight is outside the bright jet core (Dyks et al. 2006).

Several effects could lead to deviations from equation (1). The most important one is the zero time effect (t_0 effect). The t_0 effect is crucial, since when considering the multiple reactivation of the central engine, the GRB trigger time is no longer special (Zhang et al. 2006a). Every time the central engine is restarted, the new central engine time should be reset as t_0. The conventional light curves are plotted as $\log F_\nu$-$\log (t - t_{\rm trigger})$, where $t_{\rm trigger}$ is the time when the GRB triggers BAT. When we consider the emission from a late central engine activity episode, the relevant decay slope (in order to be compared with the theoretical prediction in eq. [1]) is $d \ln F_\nu / d \ln (t - t_0)$ rather than $d \ln F_\nu / d \ln (t - t_{\rm trigger})$. Properly shifting t_0 is therefore crucial to understanding the real temporal decay index in the light curves.[10] For internal dissipation models (both internal shocks or internal magnetic dissipation), the expected t_0 of a certain flare should be at the beginning of the corresponding emission episode, i.e., near the starting point of the rising segment of the flare. Since both α and β could be directly derived from the *Swift* XRT observations, this provides a solid self-consistency test to the curvature-effect interpretation and the internal origin hypothesis.

Also leading to deviations from equation (1) is the overlapping effect (Zhang et al. 2006a); i.e., there is an underlying forward shock component beneath the steep decays. In order for a clean test to the curvature effect to be performed, such a component needs to be subtracted. Kumar & Panaitescu (2000) suggested that the contribution of the external shock component is significant if the ambient density is not lower than 10^{-2} cm^{-3}.

In this paper we use the XRT data to test the curvature effect interpretation and internal origin hypothesis of the GRB prompt emission and X-ray flares. We take the GRB sample presented by O'Brien et al. (2006) and focus on the steep decay components following the prompt emission and the X-ray flares. We *assume* that the curvature effect is the cause of the steep decays, so that equation (1) is valid ubiquitously. After subtracting the underlying contribution from the forward shock, we derive the t_0 values by fitting the light curves with our model. The object is to check whether the location of t_0 is consistent with the expectation of the model, i.e., near the starting point of the relevant emission episode. The fitting model is described in § 2. The data and the fitting results are presented in § 3. Conclusions are drawn in § 4 with some discussion.

2. MODEL

The rapid decay component is our primary interest. As discussed above, we assume that this component is mainly contributed by the curvature effect. On the other hand, the overlapped contribution from an external shock component for $n > 10^{-2}$ cm^{-3} could result in a decay that would deviate significantly from equation (1) (Kumar & Panaitescu 2000). Considering both the t_0 effect and the overlapping effect, we model any steep decay component and the succeeding afterglow component with the function (Zhang et al. 2006a)

$$F_\nu(t) = A\left(\frac{t - t_0}{t_0}\right)^{-(2+\beta)} + Bt^{-C}, \tag{2}$$

where β is the X-ray spectral index during the decay, t_0 is the time zero point of the emission episode related to the decay (which in principle should be at the beginning of the rising segment of the last pulse of the prompt emission or the relevant X-ray flare if the curvature interpretation is correct), A and B are normalization parameters for both the rapid decay component and the underlying forward shock component, respectively, and C is the temporal index of the forward shock emission component. Please note that we take the zero-point time of the external shock component (afterglow) as the GRB trigger time. This has been

[10] The t_0 issue is also relevant when discussing orphan afterglows from dirty fireballs (Huang et al. 2002).

TABLE 1
THE GRB SAMPLE AND THE FITTING RESULTS

GRB[a]	Interval[b] (s)	β[c]	t_p (s)	A (ergs cm^{-2} s^{-1})	t_0 (s)	B (ergs cm^{-2} s^{-1})	C	χ^2/dof
050126.....	139–29,171	1.59(0.38)	5	$1.05(20) \times 10^{-6}$	0.18(22)	$4.62(4.46) \times 10^{-9}$	0.98(0.10)	0.71
050219A.....	111–30,460	1.02(0.20)	97	$1.23(1.35) \times 10^{-8}$	36(10)	$1.04(0.47) \times 10^{-9}$	0.62(0.05)	1.74
050315.....	134–6230	1.50(0.40)	25	$2.76(1.87) \times 10^{-9}$	62(8)	$9.22(7.63) \times 10^{-12}$	0.03(0.11)	0.87
050319.....	250–93,922	2.02(0.47)	250	$4.23(5.39) \times 10^{-11}$	167(20)	$1.07(0.28) \times 10^{-9}$	0.52(0.03)	1.09
050406.....	213–881	1.37(0.25)	213	$1.64(1.27) \times 10^{-11}$	144(12)	$4.85(0.76) \times 10^{-12}$	0(fixed)	0.06[d]
050421.....	97–473	0.27(0.37)	115	$5.08(1.83) \times 10^{-9}$	43(5)	...	...	1.54
050422.....	98.5–296,896	2.33(0.60)	53	$5.31(5.33) \times 10^{-8}$	30(5)	$1.11(0.47) \times 10^{-9}$	0.86(0.04)	0.44[e]
050502B(1)[f]	818–43,500	0.81(0.28)	758	$2.23(0.54) \times 10^{-11}$	680(16)	$1.06(2.19) \times 10^{-12}$	0.0(0.21)	1.36
050502B(2)	67,300–202,000	0.81(0.28)	73,300	$2.45(5.21) \times 10^{-11}$	19,603(11,312)	$4.99(3.52) \times 10^{-14}$	0(fixed)	0.63
050607.....	321–79,473	0.77(0.48)	321	$1.05(0.48) \times 10^{-10}$	238(13)	$4.34(2.54) \times 10^{-9}$	0.96(0.09)	0.61
050712(1).....	227–242	0.90(0.06)	227	$3.78(15.06) \times 10^{-14}$	220(9)	...	...	0.11[g]
050712(2).....	269–295	0.90(0.06)	270	$2.86(1.41) \times 10^{-11}$	208(9)	...	...	0.43[g]
050712(3).....	505–379,262	0.90(0.06)	485	$1.26(1.23) \times 10^{-12}$	440(22)	$1.40(0.49) \times 10^{-8}$	0.92(0.04)	1.67
050713A(1).....	78–98	1.30(0.07)	65	$7.30(4.55) \times 10^{-9}$	40(4)	...	...	1.21
050713A(2).....	114–154	1.30(0.07)	112	$1.08(0.23) \times 10^{-9}$	79(2)	...	...	1.5
050713A(3).....	172–230	1.30(0.07)	171	$8.90(4.70) \times 10^{-10}$	100(8)	...	...	1.59
050713B.....	150–5630	0.70(0.11)	17	$9.41(7.87) \times 10^{-8}$	31(8)	$1.94(0.44) \times 10^{-11}$	$\sim$0.01 (fixed)	1.46
050714B(1)[h]	158–393,361	4.50(0.70)	41	$2.89(10.84) \times 10^{-3}$	21(11)	$1.57(1.05) \times 10^{-9}$	0.57(0.06)	1.31
050714B(2)[i]	401–481	4.50(0.70)	400	$2.12(5.70) \times 10^{-7}$	142(39)	...	...	0.77
050716(1).....	177–345	0.33(0.03)	177	$2.08(2.85) \times 10^{-7}$	22(12)	...	...	1.34
050716(2).....	375–244,935	0.33(0.03)	383	$2.69(1.36) \times 10^{-10}$	224(22)	$2.59(1.07) \times 10^{-8}$	1.00 ± 0.04	1.18
050721.....	195–244,289	0.74(0.15)	1.5	$3.47(11.56) \times 10^{-8}$	38(37)	$2.33(0.70) \times 10^{-7}$	1.18(0.03)	1.36
050724(1).....	186–7097	0.95(0.07)	73	$2.54(1.98) \times 10^{-8}$	63(12)	$1.14(3.90) \times 10^{-8}$	1.13(0.40)	1.70
050724(2).....	70,000–99,000	0.95(0.07)	58,868	$7.25(11.08) \times 10^{-10}$	8752(4047)	...	...	0.02[g]
050730(1).....	135–201	0.33(0.08)	140	$4(75) \times 10^{-5}$	2(16)	...	...	1.00
050730(2).....	230–312	0.33(0.08)	230	$3.20(2.84) \times 10^{-9}$	95(23)	...	...	2.00
050730(3).....	435–600	0.33(0.08)	430	$1.49(0.48) \times 10^{-9}$	227(17)	...	...	1.80
050730(4).....	684–793	0.33(0.08)	680	$1.79(1.60) \times 10^{-9}$	309(69)	...	...	1.73
050730(5).....	10,000–120,000	0.33(0.08)	4700	$7.94(5.50) \times 10^{-9}$	1540(407)	...	...	2.34
050801[j]	17–109	0.72(0.54)	17	$8.62(20.93) \times 10^{-7}$	2.7(2.1)	$2.68(2.49) \times 10^{-11}$	0.1(fixed)	0.27[g]
050803.....	160–1000	0.71(0.16)	145	$2.47(1.19) \times 10^{-10}$	107(7)	$6.50(8.36) \times 10^{-10}$	0.36(0.20)	1.27
050814.....	166–58,886	1.08(0.08)	8	$2.53(0.34) \times 10^{-6}$	15(6)	$1.18(0.57) \times 10^{-9}$	0.72(0.05)	1.30
050819.....	33–11,369	1.18(0.23)	10	$1.56(3.00) \times 10^{-8}$	33(17)	$2.02(6.38) \times 10^{-11}$	0.44(0.36)	1.53
050822(1).....	165–200	1.60(0.06)	130	$2.13(1.53) \times 10^{-9}$	85(9)	...	...	1.25
050822(2).....	236–293	1.60(0.06)	238	$3.15(1.47) \times 10^{-10}$	145(8)	...	...	1.06
050822(3).....	490–16,870	1.60(0.06)	450	$6.70(1.26) \times 10^{-11}$	354(6)	$5.78(4.40) \times 10^{-11}$	0.23(0.08)	0.84

[a] The number following the burst name denotes the sequence number of the steep decay components in the light curve according to the time sequence.
[b] The time interval relative to the GRB trigger time for the data we use for the fitting, in units of seconds.
[c] Taken from O'Brien et al. (2006). These indices are derived from the spectral fitting to the overall X-ray data without considering the spectral variability.
[d] The decay part of the flare and the succeeding flat component have only four data points with large error bars. We fix the C-value and fit the data. The error of t_0 is thus small with a small reduced χ^2.
[e] If the last data point at 704,682 s is considered the reduced would be then $\chi^2 \sim 1$. This point drives most of the χ^2 values.
[f] Some observational data points of this burst have an extremely small error, say, $\Delta \log F_X < 0.1$. The χ^2 of the fitting is mostly contributed by these data points, and the reduced χ^2 is unacceptable. To make the fitting results more reasonable we take $\Delta \log F_X = 0.1$ for those data points with $\Delta \log F_X < 0.1$.
[g] These flares have few data points with large error bars. Their reduced χ^2 is too small. The fitting results are highly uncertain.
[h] Excluding the superposed X-ray flare at 331–477 s.
[i] Fit to the superposed X-ray flare at 331–477 s only.
[j] Fit to the combined BAT-XRT data in 18–110 s. The flare at $\sim$210 s does not satisfy our selection criteria (see the text).

proved by detailed numerical simulations (Lazzati & Begelman 2006; S. Kobayashi et al. 2006, in preparation).

3. DATA AND FITTING RESULTS

The *Swift* GRB sample we use is the same one presented by O'Brien et al. (2006). These are the bursts detected by *Swift* prior to 2005 October 1 for which prompt slews within 10 minutes were performed. The BAT data were processed using the standard BAT analysis software (*Swift* software vers. 2.0). The XRT data were processed using `xrtpipeline` (vers. 0.8.8). The joined BAT-XRT light curves were derived through extrapolating the BAT light curves into the XRT band (0.3–10 keV) using the joint BAT-XRT spectral parameters. For the details of the data reduction procedure we refer to O'Brien et al. (2006). For our purpose, we include only those GRBs whose XRT light curves have a steep decay component connecting to the prompt emission and those GRBs that harbor X-ray flares. In some bursts there are multiple flares, and hence, multiple steep decays. For these bursts we treat each steep decay independently. We consider only those prompt emission tails or flare tails whose decay slopes are steeper than -2 with the zero time set to the GRB trigger time. For the heavily overlapped flares in the early XRT light curves, we take only those that are well identified visually and without significant substructures. Our sample includes 36 prompt emission/flare tails from 22 GRBs, which are tabulated in Table 1. Their light curves are collected in Figure 1.

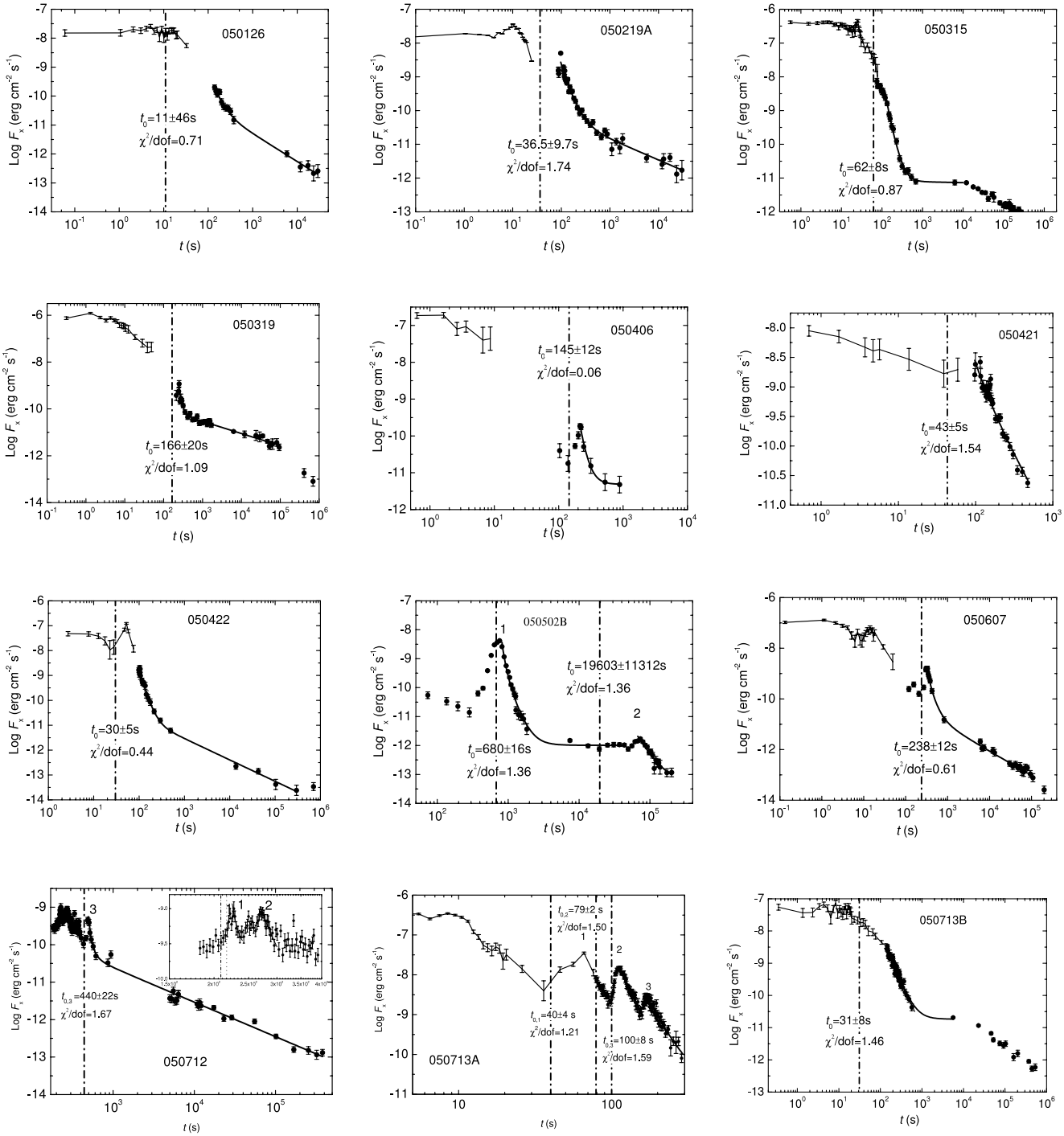

FIG. 1.—Combined BAT-XRT light curves with the best-fitting results. The connected lines with error bars are the extrapolated BAT light curves. The solid circles with error bars represent the XRT observations. The thick curves are the best fits of our model, which cover the range of the fitted data. The vertical dotted lines mark the best-fit t_0 values. When more than one steep decay component is observed, the t_0 of the ith component is denoted as $t_{0,i}$. [*See the electronic edition of the Journal for a color version of this figure.*].

Technically one needs to identify the time interval for which our above test is performed. Since the steep-decay components (the tails of the prompt emission or the X-ray flares) are required to satisfy the curvature effect, we need to search for a segment of light curve whose decay slope is steeper than -2. We choose a time window that contains four data points. We start the search from the beginning of the steep decay that follows the prompt emission or from the peak of a certain flare. We then move the time window to later times by shifting one data point in each step. We fit the decay slope for the four data points in the time window in each step until the slope becomes steeper than -2. By then the beginning of the time window is set to the starting point of the steep decay component. The end of the time interval for which our fit is performed is selected visually without a rigid criterion. For those prompt-emission/flare tails with an underlying shallow decay (afterglow) component, we take the end of that component (before a further break if any) as the end of the time interval and fit the data using equation (2). For some tails without the superposition of an underlying afterglow component or that are otherwise highly overlapped with other flares, we simply choose the

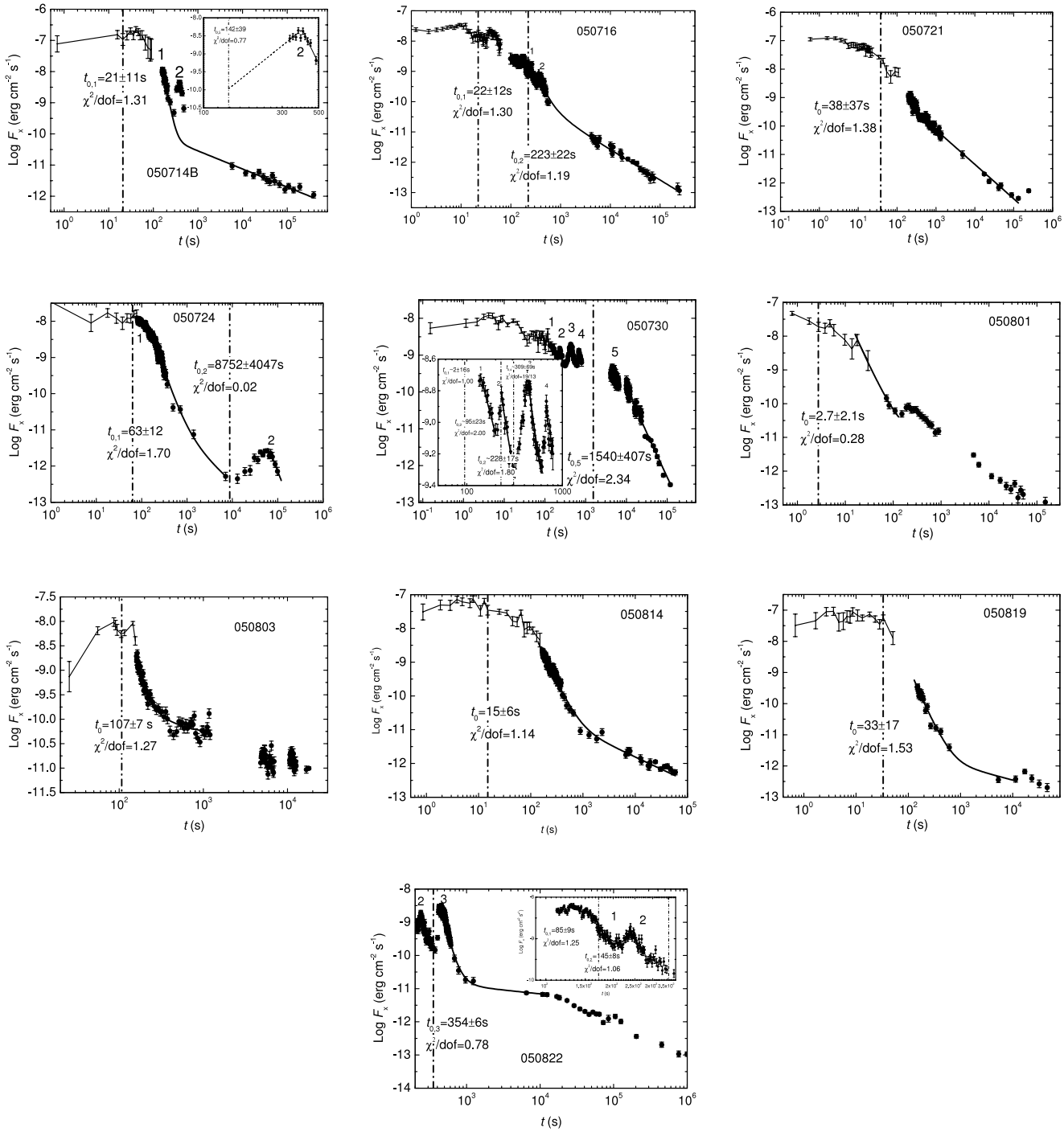

Fig. 1.—*Continued*

last data point of the steep decay component as the end of the time interval and fit the light curve using equation (2) by setting $B = 0$.

The GRBs 050406, 050502B, 050713B, and 050801 have a very flat segment following the tails of the prompt emission or flares. These flat segments have only a few data points, and we fix the C-values in our fitting for these GRBs. Several bursts, e.g., GRBs 050712 (the first and the second flares), 050713A, 050716 (the first flare), 050730 (the first through fourth flares), and 050822 (the first and second flares), have heavily overlapped flares before the typical long tail, as observed in many other GRBs (050126, 050219, 050315, etc.). We also fit these flares. The XRT light curve of GRB 050714B has a rapid flare in the tail segment. The level of this flare is significantly higher than the tail. We subtract the flare from the tail segment and fit the tail segment and the flare independently.

The spectral indices we use are from O'Brien et al. (2006). These spectral indices are derived from the spectral fitting to the overall X-ray data without spectral variability being considered. In principle one should use the β-value during the steep decay to perform the test. However, the photon counts during the steep decay only are usually too low to give a high significance fit. The X-ray spectra of some GRBs, such as GRB 050502B (Falcone et al. 2006) and GRB 050607 (Pagani et al. 2006), have detectable

spectral variability. We check the difference made by this effect with GRB 050502B and find that it does not significantly affect our fitting results. Throughout this analysis we use the spectral indices from O'Brien et al. (2006).

Our fitting results are summarized in Table 1. In Figure 1, we mark the time interval of the fitting data and the fitting curve by solid lines, and indicate the fitted t_0 of each steep decay component by a vertical dash-dotted line. For those light curves with multiple tail/flares, we identify the t_0 of the ith steep decay component as $t_{0,i}$. The reduced χ^2 of the fits are also shown in Figure 1.

From Figure 1 we find that, except those heavily overlapped flares in the early XRT light curves, the fitted t_0 values of a good fraction of the well-identified tails are right at the beginning of the rising phase of the flare or the last pulse of the prompt emission. These include GRBs 050126, 050219A, 050319, 050406, 050422, 050502B (the late flare), 050607, 050712 (the third flare), 050716 (the second flare), 050724 (the late flare), 050803, and 050822 (the third flare). This is well consistent with our starting hypothesis, i.e., that the flares are of internal origin and mark the reactivations of the central engine (Zhang et al. 2006a). We emphasize that the fitted t_0 values are based on the hypothesis of the curvature effect as the origin of the steep decay, which is only relevant to internal models, not to external ones. So even if some external models may also allow t_0 to be reset before the flares, the decay slope after the peak would follow some other predictions [typically flatter than $-(2+\beta)$; e.g., Wu et al. 2006]. As a result, the fitted t_0 values to satisfy those predictions would be significantly different from the ones we obtained, i.e., they should have a large offset with respect to the rising part of the flare. This means that one does not find a self-consistent solution for the external shock models. The impressive consistency displayed in the above bursts lends strong support to the internal origin of these X-ray flares. It is worth noticing that a very late flare ($\sim$1 day) is evident in the XRT light curves of GRB 050502B (Falcone et al. 2006) and the short burst GRB 050724 (Barthelmy et al. 2005a). There have been questions as to whether the central engine can restart at such a late epoch and whether these features are due to a refreshed external shock origin (e.g., Panaitescu et al. 1998; Zhang & Mészáros 2002). Our results indicate remarkably that the t_0 values for these two late flares are also right before the rising part of the flares. This gives strong support to the internal origin of these flares and calls for central engine models that can operate as long as $\sim$1 day.

The fitted t_0 values for some tails in GRBs 050315, 050712, 050713A, 050714B, 050716, 050721, 050724, 050730, 050801, 050814, 050819, and 050822 are all before the peak of the corresponding flare or the starting point of the steep decay. However, they are apparently not located at the rising part of a flare or prompt emission pulse. These are all highly overlapping flares or continuously decreasing prompt emission, so that the rising segment of the flare or the prompt emission pulse is deeply buried beneath the continuous emission. These cases do not contradict the internal models and the curvature effect interpretations, although they do not directly support the scenario. Further complications may come from the possibility that the electron injection does not cease abruptly, that the observational band is below the cooling frequency, and that spectral breaks may cross the band during the decay, etc. In any case, these findings confirm that it is difficult to search for evidence of the curvature effect using the prompt GRB light curves. On the other hand, if one believes the internal origin and curvature effect scenario (as is self-consistently tested in other bursts), then the fitted t_0 values in these bursts give some indication of the central engine time when the flare or the last pulse of the prompt emission is powered.

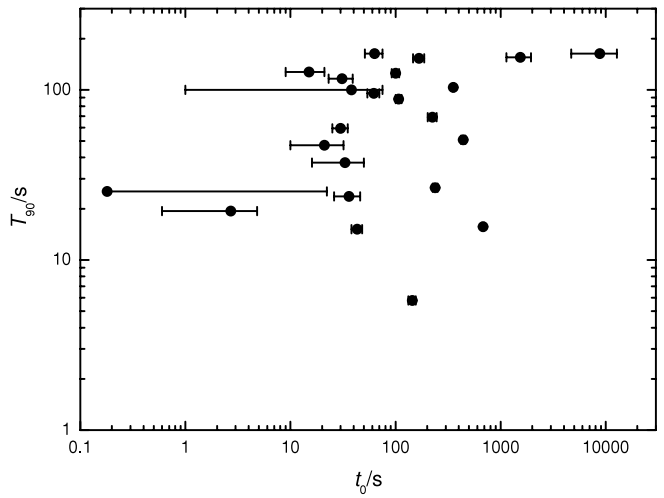

FIG. 2.—Value of t_0 as a function of T_{90} for the tails/flares in our sample, except for those heavily overlapped flares in the early-time XRT light curves.

In Figure 2, we display the fitted t_0 values as a function of T_{90}, the duration of the prompt emission. The cases of heavily overlapped flares are not included. It is found that the two quantities are not correlated, indicating that the onset time of the late central engine activity does not depend on the duration of the prompt central engine activity. This suggests irregular, unpredictable behaviors of the GRB central engine.

We have used the light curve in the observer's frame to perform the above fits. Using the intrinsic light curves [i.e., systematically changing the time axis to the cosmic proper frame time $t/(1+z)$] shifts the searched time zero point to $t_0/(1+z)$. So our conclusion does not depend on the time dilation effect, since the light curves are simply compressed in the cosmic proper frame.

4. CONCLUSIONS AND DISCUSSION

We have analyzed 36 prompt emission/flare tails in the XRT light curves of 22 GRBs detected by *Swift* before 2005 October 1 that show clear steep decay components. This is a subsample of that presented by O'Brien et al. (2006). Assuming that the tails are predominantly caused by the curvature effect, we derive the t_0 values of these tails by fitting the XRT light curves with equation (2). Our results (Fig. 1 and Table 1) suggest that usually the t_0 values are near the beginning of the rising segment of the last pulse of the prompt emission or the corresponding X-ray flare, which is consistent with the expectation of the internal dissipation models for the prompt emission and X-ray flares (e.g., Burrows et al. 2005; Zhang et al. 2006a; Fan & Wei 2005; Ioka et al. 2005; Falcone et al. 2006; Romano et al. 2006). This suggests that the GRB central engine reactivates after the early prompt emission is over, sometimes up to days after the trigger (e.g., GRB 050502B and GRB 050724). This finding challenges the conventional central engine models and calls for new ideas about how restart the central engine is restarted (e.g., King et al. 2005; Perna et al. 2006; Fan et al. 2005; Proga & Zhang 2006; Dai et al. 2006). We also show that the onset times of the late central engine activity do not depend on T_{90}, suggesting an erratic, unpredictable central engine.

About one-third of the light curves in the O'Brien et al. (2006) sample do not show a distinct steep decay component that connects the prompt emission and the afterglow. It is possible that in some GRBs (e.g., GRB 050525A; Blustin et al. 2006) the XRT observations started too late to catch the prompt emission tail. Nonetheless, a small fraction of XRT light curves show an apparently smooth transition from the prompt emission to the afterglow

emission without a steep decay bridge. The most prominent cases are GRB 050401 (De Pasquale et al. 2006), 050717 (Krimm et al. 2006), and 050826 (O'Brien et al. 2006). The joined BAT-XRT light curves of these GRBs (see O'Brien et al. 2006) have some low-amplitude flares overlapping on an otherwise smooth single power-law decay component extending to a late epoch. If these light curves are still interpreted within the frame work of internal-external model, as is favored by the majority of bursts in the sample (Fig. 1), the prompt emission and the flares are of internal origin, with a smaller emission efficiency than most other bursts (Zhang et al. 2006b). For example, the light curve of GRB 050717 could be also well modeled by the superposition of a prompt emission tail emission and an underlying afterglow component (Krimm et al. 2006). Alternatively, it may be possible that the fireball in these cases is decelerated at a very early time so that both the prompt emission and the afterglow originate from the external shocks (e.g., Dermer & Mitman 1999, 2004). This scenario requires a high ambient density and a high initial Lorentz factor of the fireball. The low-amplitude flares overlapping on the decaying light curves could be still from late internal dissipation of the central engine or from some external shock-related collisions (Wu et al. 2006), or else they could result from possible density clumps in the medium (e.g., Dermer & Mitman 1999; 2004).

We thank Z. G. Dai, Y. F. Huang, D. A. Kahn, D. Kocevski, J. Norris, and X. F. Wu for useful discussion/comments. This work is supported by NASA under grants NNG05GB67G, NNG05GH92G, and NNG05GH91G (B. Z. and E. W. L.), and the National Natural Science Foundation of China (grant 10463001 to E. W. L.).

REFERENCES

Barthelmy, S. D., et al. 2005a, Nature, 438, 994
———. 2005b, ApJ, 635, L133
Blustin, A. J., et al. 2006, ApJ, 637, 901
Burrows, D. N., et al. 2005, Science, 309, 1833
Cusumano, G., et al. 2006a, Nature, 440, 164
———. 2006b, ApJ, 639, 316
Dai, Z. G., Wang, X. Y., Wu, X. F., & Zhang, B. 2006, Science, 311, 1127
Daigne, F., & Mochkovitch, R. 1998, MNRAS, 296, 275
De Pasquale, M., et al. 2006, MNRAS, 365, 1031
Dermer, C. 2004, ApJ, 614, 284
Dermer, C., & Mitman, K. E. 1999, ApJ, 513, L5
———. 2004, in ASP Conf. Ser. 312, Third Rome Workshop on Gamma-Ray Bursts in the Afterglow Era, ed. M. Feroci, F. Frontera, N. Masetti, & L. Piro (San Francisco: ASP), 301
Drenkhahn, G., & Spruit, H. C. 2002, A&A, 391, 1141
Dyks, J., Zhang, B., & Fan, Y. Z. 2006, ApJ, submitted (astro-ph/0511699)
Falcone, A., et al. 2006, ApJ, 641, 1010
Fan, Y. Z., & Wei, D. M. 2005, MNRAS, 364, L42
Fan, Y. Z., Zhang, B., & Proga, D. 2005, ApJ, 635, L129
Fenimore, E., Madras, C. D., & Nayakshin, S. 1996, ApJ, 473, 998
Fox, D. B., et al. 2005, Nature, 437, 845
Gehrels, N., et al. 2004, ApJ, 611, 1005
———. 2005, Nature, 437, 851
Giannios, D., & Spruit, H. C. 2006, A&A, 450, 887
Huang, Y. F., Dai, Z. G., & Lu, T. 2002, MNRAS, 332, 735
Ioka, K., Kobayashi, S., & Zhang, B. 2005, ApJ, 631, 429
King, A., O'Brien, P. T., Goad, M. R., Osborne, J., Olsson, E., & Page, K. 2005, ApJ, 630, L113
Kobayashi, S., Piran, T., & Sari, R. 1997, ApJ, 490, 92
Kocevski, D., Ryde, F., & Liang, E. 2003, ApJ, 596, 389
Krimm, H. A., et al. 2006, ApJ, in press (astro-ph/0605507)
Kumar, P., & Panaitescu, A. 2000, ApJ, 541, L51
Lazzati, D., & Begelman, M. C. 2006, ApJ, 641, 972
Mészáros, P., & Rees, M. J. 1997, ApJ, 476, 232
Norris, J. P. 2002, ApJ, 579, 386
Nousek, J. A., et al. 2006, ApJ, 642, 389
O'Brien, P. T., et al. 2006, ApJ, in press (astro-ph/0601125)
Pagani, C., et al. 2006, ApJ, in press (astro-ph/0603658)
Panaitescu, A., Mészáros, P., Gehrels, N., Burrows, D., & Nousek, J. 2006, MNRAS, 366, 1357
Panaitescu, A., Mészáros, P., & Rees, M. J. 1998, ApJ, 503, 314
Perna, R., Armitage, P. J., & Zhang, B. 2006, ApJ, 636, L29
Piro, L., et al. 2005, ApJ, 623, 314
Proga, D., & Zhang, B. 2006, MNRAS, in press (astro-ph/0601272)
Qin, Y.-P., & Lu, R. J. 2005, MNRAS, 362, 1085
Qin, Y.-P., et al. 2004, ApJ, 617, 439
———. 1994, ApJ, 430, L93
Romano, P., et al. 2006, A&A, 450, 59
Roming, P. W. A., et al. 2006, ApJ, submitted (astro-ph/0509273)
Ryde, F., & Petrosian, V. 2002, ApJ, 578, 290
Sari, R., & Piran, T. 1997, ApJ, 485, 270
Sari, P., Piran, T., & Narayan, R. 1998, ApJ, 497, L17
Shen, R. F., Song, L. M., & Li, Z. 2005, MNRAS, 362, 59
Tagliaferri, G., et al. 2005, Nature, 436, 985
Thompson, C. 1994, MNRAS, 270, 480
Usov, V. V. 1992, Nature, 357, 472
Vaughan, S., et al. 2006, ApJ, 638, 920
Wu, X. F., et al. 2006, ApJ, submitted (astro-ph/0512555)
Yamazaki, R., Toma, K., Ioka, K., & Nakamura, T. 2006, MNRAS, in press (astro-ph/0509159)
Zhang, B., Fan, Y. Z., Dyks, J., Kobayashi, S., Mészáros, P., Burrows, D. N., Nousek, J. A., & Gehrels, N. 2006a, ApJ, 642, 354
Zhang, B., & Mészáros, P. 2002, ApJ, 566, 712
———. 2004, Int. J. Mod. Phys. A, 19, 2385
Zhang, B., et al. 2006b, ApJ, submitted